View Article Online / Journal Homepage / Table of Contents for this issue

Enhanced electrorheology of suspensions containing sea-urchin-like hierarchical Cr-doped titania particles†

Jianbo Yin, Xiaopeng Zhao,* Liqin Xiang, Xiang Xia and Zhanshu Zhang

Received 26th May 2009, Accepted 21st August 2009
First published as an Advance Article on the web 22nd September 2009
DOI: 10.1039/b910274d

Published on 22 September 2009. Downloaded by Pennsylvania State University on 16/09/2016 13:48:09.

We developed a novel electrorheological (ER) suspension composed of Cr-doped titania particles with a sea-urchin-like hierarchical morphology, and demonstrated a distinct enhancement in ER properties. These hierarchical ER particles, which are easy to synthesize by a solvothermal approach, are nearly monodisperse and consist of high-density rutile Cr-doped titania nanorods assembled radially on the surfaces of particles. The specific surface area of the hierarchical Cr-doped titania particles is $\sim$ 65 m^2/g, which is higher than that (5 m^2/g) of the smooth non-hierarchical Cr-doped titania particles. Under electric fields, the ER properties of the suspension containing such hierarchical particles are investigated by steady shear viscosity and dynamic viscoelastic experiments. It is found that the suspension of hierarchical Cr-doped titania particles possesses a stronger ER effect compared to the corresponding suspension of smooth non-hierarchical Cr-doped titania particles. Its yield stress and ER efficiency are approximately twice as high as those of the smooth Cr-doped titania suspension. Meanwhile, a higher ER effect is also demonstrated for the hierarchical pure titania suspension in comparison with the smooth pure titania suspension. Furthermore, under electric and shearing fields the rheological and structuring processes of the hierarchical particle suspension is significantly different from that of the smooth particle suspension. In terms of the dielectric analysis and microscopy observation, the enhancement of ER effect of the suspension of hierarchical Cr-doped titania is likely attributed to the combined effects including improved interfacial polarization and increased interparticle interaction due to the presence of urchin-like nanostructures on the ER microparticles.

1. Introduction

Recently, there has been increasing interest in the morphological control of functional materials because there is a close relationship between the morphology and properties.[1–3] In particular, introducing nano-scale structures onto micro-scale materials has stimulated much attention since such micro/nano-hierarchical materials often combine the features of micro- and nano-scale building blocks and show unique properties that are different from those of mono-morphological materials.[4] This strategy is generally considered to originate from the inspiration of hierarchically biological structures in nature. For instance, the claw of a gecko is a classic hierarchical structure, consisting of microscopic hairs called setae, which further split into hundreds of smaller nanometre-size structures called spatulas. When the claw of a gecko makes contact with any surface, the nanometre-size spatulas enable molecular contact over large areas and thus translate weak van der Waals interactions into enormous attractive forces by association with micrometre-length scales of the setae.[5,6] Up to now, many functional materials with a unique hierarchical morphology have been studied for various applications such as photocatalysts,[7] sensors,[8] electrodes,[9] *etc.* However, the use of materials with a unique hierarchical morphology in an electrorheological (ER) fluid, a kind of smart complex fluid capable of varying viscosity or even solidification by external electric fields, has found considerably less attention although the morphology of dispersed particles has been considered to be one of the important factors to influence ER properties.[10–12]

ER fluids consist of polarizable solid particles with high relative dielectric constants dispersed in a non-conducting liquid with a relatively low dielectric constant. When an external electric field is applied, ER fluids exhibit drastic and reversible changes in rheological properties due to the field-induced ordering of the particulate phase.[13] Especially, the rheological changes can be accurately controlled by tuning electric field strengths. This simple electric-controlled mechanical response makes ER fluids possess many potential applications in various devices such as dampers, brakes, actuators, and so on.[14,15] Regarding these applications, ER fluids with versatile performances, including high yield stress or ER efficiency, wide temperature range, dispersion stability, low no-field viscosity, *etc.* are especially needed. The past decades have witnessed huge activities concerning the preparation of ER materials. Various materials, such as zeolites,[16] modified titania,[17] titanates,[18] carbonous,[19] polar and semi-conducing polymers,[20] core–shell particles,[21] nanocomposites,[22,23] mesoporous particles,[24,25] have been studied for ER applications. However, the practical

Institute of Electrorheological Technology, Department of Applied Physics, Northwestern Polytechnical University, Xi'an, 710072, China. E-mail: xpzhao@nwpu.edu.cn; Fax: +86-29-88491000; Tel: +86-29-88431662

† Electronic supplementary information (ESI) available: SEM images of pure titania particles with urchin-like hierarchical morphology; N_2 adsorption-desorption isotherms; SEM image of Cr-doped titania particles with a changed surface morphology; frequency dependence of storage modulus and loss modulus of pure titania particles suspensions; stress dependence of storage modulus and loss modulus of pure titania particles suspensions. See DOI: 10.1039/b910274d

View Article Online

Published on 22 September 2009. Downloaded by Pennsylvania State University on 16/09/2016 13:48:09.

applications of ER fluids are still hampered up to now by either low yield stress, temperature instability or particle sedimentation.

Since the ER effect is induced by an external electric field, the particle polarization and the interaction between particles are believed to play an important role and the dielectric properties should be critical.[14a,26] Thereby, in the synthesis of ER materials, more studies focus on the intrinsic structure and composition of particles because the polarization or dielectric properties depended on them directly. Titania is a well-known ER material which has been presumed to have high ER activity due to its high dielectric constant but actually shows a very weak ER effect.[27,28] Having considered the influences of intrinsic structure and composition on polarization or dielectric properties, we had proposed a way to increase the ER activity of titania by doping with metal ions.[17] The yield stress of the doped titania ER fluid was found to increase by about 10 times more than that of the pure titania ER fluid. The modifications of dielectric properties, which had been attributed to the activated internal structure by doping, were verified to be responsible for the ER improvement.[17,28b] On the other hand, besides the composition and structure, the morphology of ER particles is also considered to be a critical factor influencing ER performance.[10,29] Many researchers have theoretically and experimentally investigated the effect of morphology on ER properties, but most of studies are mainly focused on the simple shape or size effect, such as using elongated or fiber-like particles as ER dispersal phases.[10,11,30] Recently, nano-size particles have been used to develop new ER fluids.[31] The obtained high yield stress showed the potential of nanomaterials for ER systems. However, the ER fluids based on nanoparticles also subjected to some disadvantages such as high no-field viscosity and shear instability.[32] It is well known that the hierarchical structure is one of the important forms among various morphologies, which a unique structure is made up of building units at different levels.[33] In particular, the micro/nano hierarchical structures have been frequently adopted in advanced functional materials. A previous study in our lab has given a preliminary investigation about the ER property of a kind of micro/nano-structured clay–titanate composite.[34] However, it was found that the clay was easily destroyed by the strong base medium in the reaction, which resulted in the difficulty of morphology control and reproduction. Thus, the substantial contribution from the micro/nano-structure was negligible because the particle composition and structure were different between the micro/nano-structured composite and the original clay or clay–titania composite.

In this work, we developed a novel ER suspension composed of Cr-doped titania particles with unique sea-urchin-like hierarchical architectures. These hierarchical ER particles are easily synthesized by a solvothermal approach and show characteristics including nearly monodisperse and well-defined morphology and structures. Under electric fields, the rheological properties of the suspension containing such hierarchical particles were investigated in detail and compared with the corresponding suspension containing smooth non-hierarchical Cr-doped titania particles that had a similar crystal structure and composition with the hierarchical particles. It was demonstrated that not only doping but also introducing nanostructure into ER particles largely enhanced the ER effect. The structurally enhanced ER effect was further discussed based on the investigation about dielectric properties and microscopic ER structures.

2. Experimental

Synthesis of ER particles

Sea-urchin-like hierarchical Cr-doped titania particles. 4.0 mL of titanium tetrabutyl titanate (TBT, analytical, Kermel Chemical Reagent Co. Ltd of China) was dissolved in 30.0 mL of methylbenzene to form a transparent solution. Then, 0.6 g of $CrCl_3 \cdot 7H_2O$ (analytical, Sinopharm Chemical Reagent Co. Ltd of China) was dissolved in 4.0 mL of 3 M titanium chloride (analytical, Sinopharm Chemical Reagent Co. Ltd of China) aqueous solution and the resulting solution was added dropwise into the above TBT/methylbenzene solution. After string for 1 h precipitates were formed, which were transferred, in solution, into a Teflon-lined autoclave. After heating at 150 °C for 72 h, the precipitates were isolated by filtration, washed with ethanol, and dried at 80 °C for 12 h. Finally, the dried particles were heated at 600 °C to remove residual organics to obtain the sea-urchin-like hierarchical Cr-doped titania particles as shown in Fig. 1a,b. The hierarchical pure titania particles were synthesized by the same process while no dopant was added.

Smooth non-hierarchical Cr-doped titania particles. The non-hierarchical Cr-doped titania particles with smooth surfaces were prepared by a modified sol–gel-hydrothermal reaction of TBT solution containing the required amount of Cr(III) in the presence of a surfactant or copolymer as described in ref. 35. Typically, 4 g of PEG 400 (analytical, Sinopharm Chemical Reagent Co. Ltd of China) was added into 90 mL of ethanol containing 5 g of TBT and $CrCl_3 \cdot 7H_2O$ (Cr/Ti = ~3 mol%) with stirring to form a transparent solution. Then, 10 mL of ethanol containing a small amount of distilled water was added into the above solution under the protection of flowing nitrogen. The resulting solution was further stirred for several minutes until it suddenly became opaque. This suspension was quietly aged for 24 h at 35–40 °C to form precipitates. The precipitate was transferred

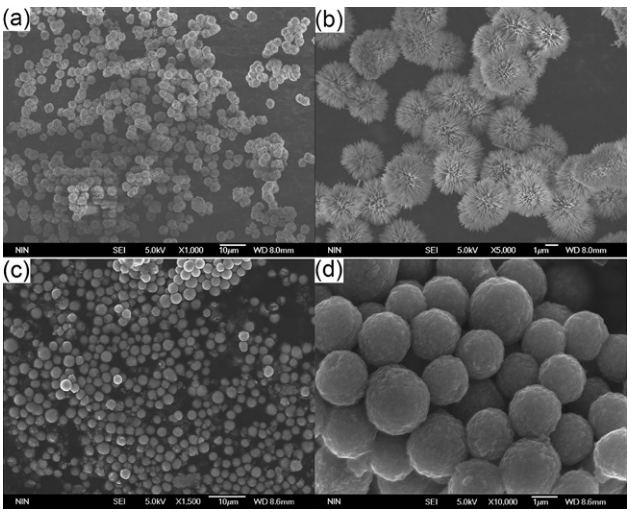

Fig. 1 SEM images of sea-urchin-like hierarchical Cr-doped titania particles (a, b) and smooth Cr-doped titania particles (c, d).

 This journal is © The Royal Society of Chemistry 2009

View Article Online

Published on 22 September 2009. Downloaded by Pennsylvania State University on 16/09/2016 13:48:09.

into a Teflon-lined autoclave and heated at 150 °C for 72 h. After, the precipitate was separated by filtration, washed by ethanol, and dried at 80 °C for 12 h. Finally, the dried particles were heated at 600 °C to obtain the smooth non-hierarchical Cr-doped titania particles as shown in Fig. 1c,d. The smooth pure titania particles were also synthesized by the same process while no dopant was added.

Characterization

The morphology of the particles was observed by scanning electron microscopy (SEM, JSM-6700) and transmission electron microscopy (TEM, JEOL-3010). The particle size distribution was determined by a laser scatter particle size analyzer (LS230, Beckman Coulter) (dispersing the particles in ethanol). The crystal structure was determined by powder X-ray diffraction patterns (XRD, Philips X'Pert Pro X-ray diffractometer) with Cu Ka irradiation at 40 kV/35 mA. The chemical composition and valence were analyzed by an energy-dispersive spectrum (TEM/EDS, JEOL-3010) and X-ray photoelectron spectroscopy (XPS, Axis Ultra, Kratos) with a monochromatic Al K_α source. The EDS measurement was made by focusing an electron beam into a ~10 nm diameter spot on different locations of particles to precisely determine the Cr/Ti ratio. The C1s peak at 284.6 eV of the surface adventitious carbon was referred for all the binding energies in XPS. The BET surface areas were obtained by the N_2 adsorption isotherm (Nova 2000e surface area & pore size analyzer, Quantachrome). All samples were degassed at 200 °C under vacuum for a minimum of 6 h.

Preparation of ER suspensions

Before preparing ER suspensions, the particles were dehydrated in a vacuum drum dryer (0.085 MPa) at 150 °C for 8 h. Meanwhile, a DHS-20 infrared moisture analyzer was used to detect moisture in particles and the result showed that there was almost no moisture after dehydration under vacuum. Then, the dried particles (dielectric constant of ~70 for hierarchical Cr-doped titania, of ~64 for smooth Cr-doped titania, ~ 36 for hierarchical pure titania, and ~ 32 for smooth pure titania, which was determined by impedance analyzer (HP4284A) at 1 kHz using a test fixture (HP16451B) for solid plates compressed at 10 MPa) were mixed immediately with silicone oil (dielectric constant of 2.7–2.9, viscosity of 50 mPa s, density of 0.998–1.005 g/cm^3 at 25 °C) to produce ER suspensions. The particle fraction was defined by the ratio of particle volume to total volume of suspension. In order to mix particles with oil sufficiently, the suspensions were further stirred for 1 h and then heated for 2 h at 150 °C again. The IR spectra (FT-IR, JASCO FT/IR-470 Plus) of suspensions, done by daubing on KBr crystals, showed no peaks at around 3400 cm^{-1} and 1650 cm^{-1} due to water. Therefore, it was considered that the amount of absorbing moisture was too small to influence the ER properties of samples. Furthermore, in order to clarify the influence of surface morphology on ER properties rationally, no surfactant or other additives were added to the suspensions because they possibly affected ER properties.[14,15] Although the particle settling readily occurred for titania suspensions due to a large density mismatch, we noted that it did not influence the ER measurements and data comparison because the ER measurements were finished in a relatively short period. In this short measurement period, no suspension sedimentation was observed, in particular under the influences of electric and shearing fields.

Electrorheological measurements

The ER properties were characterized by steady-shearing viscosity and dynamic viscoelastic experiments at room temperature on a controlled stress rheometer (Thermal-Haake RS600) with a plate–plate system (PP ER35, the gap between plates was 1.0 mm.), a dc high-voltage generator (10 kV/2 mA, WYZ-010), a thermocontroller (oil bath, −25 – +125 °C, Phoenix), and a PC computer. In the steady shearing experiment, the flow curves of shear stress or shear viscosity–shear rate were measured by the controlled shear rate (CSR) mode within 0.1–1000 s^{-1} (note that there was no sample migration or expulsion even at 1000 s^{-1}). Prior to each measurement, we pre-sheared the suspensions for two minutes at 300 s^{-1} and then applied electric fields. Each shear rate was maintained for a time high enough (30 s for 0.1–10 s^{-1} and 10 s for 10–1000 s^{-1}. The time was determined by the shear stress–time curves at some typical fixed shear rates) to ensure that the stationary state was reached. The yield stress was approximately obtained at the low shear rate or by an extrapolation of the curly course of the shear stress to zero shear rates. The dynamic viscoelastic properties were measured as a function of stress at a constant frequency and as a function of frequency at a constant stress in the linear regions. In this process, the amplitude sweep test of modulus as a function of stress at a constant frequency (0.5 Hz) was initially attempted to find a linear viscoelastic region, and then the dynamic viscoelastic properties were measured as a function of frequency at a stress in the linear regions. To make an equivalent comparison, the same frequency and stress were chosen for smooth and hierarchical titania ER suspensions and the electric field was applied for one minute prior to applying sweeping. Each measurement was repeated at least three times to ensure data consistency.

Dielectric measurements and microscopic observation

The dielectric spectra of ER suspensions were measured by an impedance analyzer (HP4284A) within the frequency range from 20 Hz to 1 MHz using a test fixture (HP16452A) for liquids to investigate their interfacial polarization. The 1 V of bias electrical potential was applied to ER suspensions during measurement. It was small so that no chain formation within ER suspensions was induced, thus we could obtain the true behavior of the interfacial polarization between particles and medium and well compare the dielectric properties.[24c]

The ER structures formed between two electrodes were captured by an *in-situ* optical observation with a CCD camera, while the microstructure of chains formed by particles was further observed by scanning electron microscopy (SEM). In the SEM observation, the particles were suspended in a drop of dimethybenzene and a planar electric field was applied across the droplet. The droplet was then allowed to evaporate while the applied field was maintained. This allowed for the direct examination of the approximate on-state structure.[12c]

View Article Online

Published on 22 September 2009. Downloaded by Pennsylvania State University on 16/09/2016 13:48:09.

3. Results and discussion

Structural characteristics

The morphology of the Cr-doped titania particles is shown by SEM images in Fig. 1. It was found that the particles synthesized by the solvothermal process are sea-urchin-like hierarchical microspheres that comprise numerous 1D nanorods grown radially on the surfaces of the spheres (Fig. 1a, b). These hierarchical microspheres are separated and nearly monodisperse with a mean particle size of 3.2 μm according to the LS particle size analysis. The diameter of nanorods is about 20–30 nm observed by the high-resolution TEM images as shown in Fig. 2. The non-doped particles synthesized by the same solvothermal process also show a similar sea-urchin-like hierarchical morphology but their sizes are slightly smaller than that of the Cr-doped ones and the size distribution becomes broad (see Fig. S1, ESI†). The particles obtained by the sol–gel-hydrothermal method are uniform non-hierarchical microspheres whose surface is approximately smooth (Fig. 1c, d) and the mean diameter of the smooth pure titania and doped titania is 2.8 μm and 2.3 μm, respectively.

The crystal structure of the samples was determined by XRD patterns, shown in Fig. 3. Both the smooth and hierarchical pure titania particles exhibit a rutile phase and a small amount of anatase phase. However, the Cr-doped titania shows the rutile phase only, indicating that doping with Cr ions promotes the formation of the rutile phase. This may be attributed to the increased concentration of oxygen vacancy defects in the titania lattice due to the Cr^{3+} (confirmed by XPS) doping in titania according to the previous reports.[36] Furthermore, no peaks originating from separate phases such as chromic or other chromium-containing crystalline phase oxides are detected from the Cr-doped titania. The typical XRD peak ascribed to the (110) reflection of rutile shows a very slight shift from a *d*-spacing of 3.235 Å of the hierarchical pure titania to 3.247 Å of the hierarchical Cr-doped titania. Similarly, the (110) reflection of the smooth doped titania is slightly shifted to 3.246 Å from 3.236 Å of the smooth pure titania. These hint that some Cr ions may be incorporating into the lattice of titania and producing a slight expansion of framework possibly because of the formation of oxygen vacancy defects when Cr^{3+} (0.615 Å) substitutes Ti^{4+} (0.605 Å).[36]

The compositions and chemical states of elements are analyzed by EDS and XPS spectra as shown in Fig. 4 and 5. The EDS

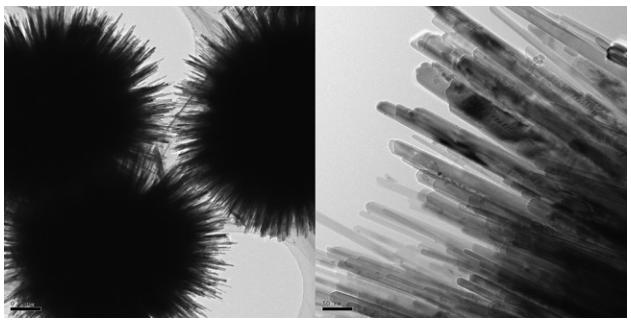

Fig. 2 TEM images of sea-urchin-like hierarchical Cr-doped titania particles (scale bar = 500 nm (left) and 50 nm (right)).

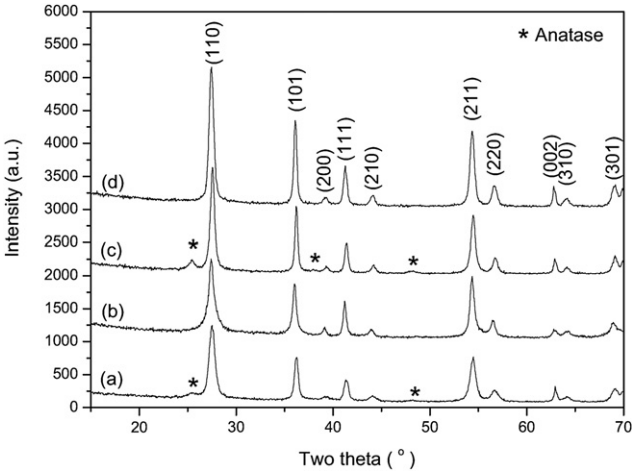

Fig. 3 XRD patterns of samples: (a) smooth pure titania particles; (b) smooth Cr-doped titania; (c) hierarchical pure titania particles; (d) hierarchical Cr-doped titania particles.

results in Fig. 4 show that both the hierarchical and smooth Cr-doped titania particles contain Cr/Ti elements (O element is verified by XPS in Fig. 5). No other extraneous metal elements are detected. (The signals of Cu are from the copper grid used.) The mole ratio of Cr to Ti in the hierarchical Cr-doped titania particles is 2.88 mol%, which is much lower than the original concentration ratio in the precursor solution. This is likely because of the doping limit that makes more Cr ions fail to incorporate into titania.[36a,37] For comparison, the Cr/Ti ratio in

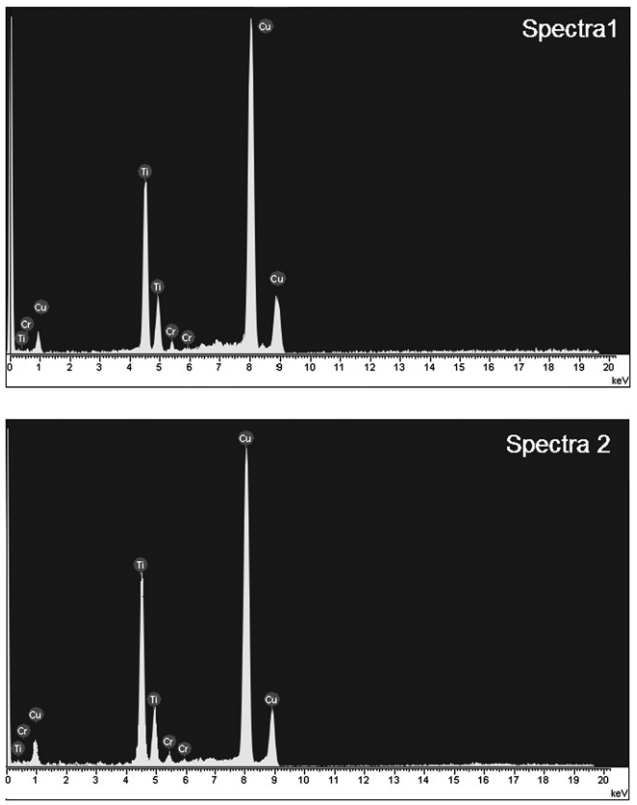

Fig. 4 EDS spectra of hierarchical Cr-doped titania particles (spectra 1) and smooth Cr-doped titania particles (spectra 2).

 This journal is © The Royal Society of Chemistry 2009

View Article Online

Published on 22 September 2009. Downloaded by Pennsylvania State University on 16/09/2016 13:48:09.

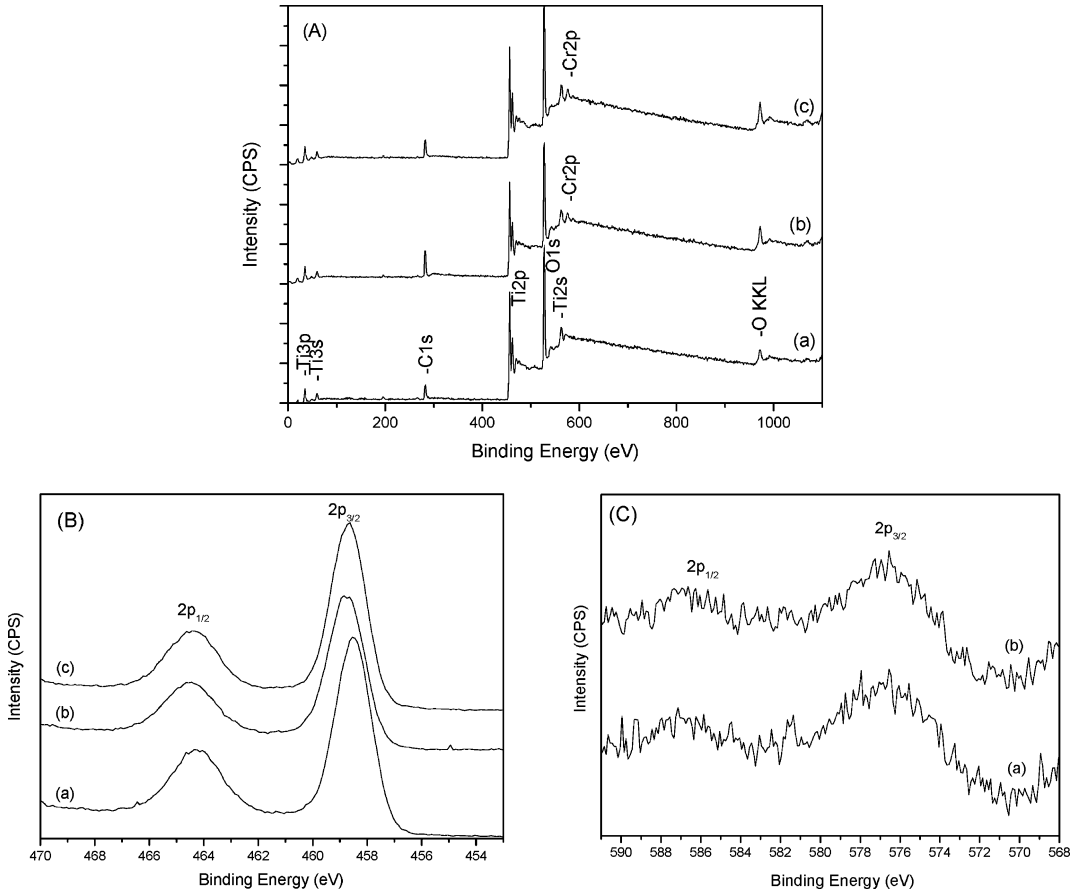

Fig. 5 XPS spectra of particles (A) survey: (a) hierarchical pure titania, (b) hierarchical Cr-doped titania, (c) smooth Cr-doped titania; (B) Ti2p peaks: (a) hierarchical pure titania, (b) hierarchical Cr-doped titania, (c) smooth Cr-doped titania; (C) Cr2p peaks: (a) hierarchical Cr-doped titania, (b) smooth Cr-doped titania.

the smooth Cr-doped titania particles is also controlled to ~3 mol% (EDS result is 2.92 mol%) by adjusting the original concentration ratio, which is close to that in the hierarchical Cr-doped titania particles. The XPS spectra in Fig. 5 further confirms that the hierarchical and smooth Cr-doped titania particles both contain only Ti, O, and Cr. (The trace amount of carbon is from the adventitious hydrocarbon in air, which is also observed in all samples). The Cr/Ti ratio, determined from the ratio of XPS peak areas corrected with the empirical sensitivity factors, is 3.01 mol% for the hierarchical Cr-doped titania particles and 3.06 mol% for the smooth Cr-doped titania particles, respectively. Note that this Cr/Ti ratio is very close to that obtained by the EDS, further indicating that most of the Cr ions might have been incorporated into titania rather than adsorption on the surface of the crystal because XPS is usually used to determine the surface elements. Furthermore, the high-resolution XPS spectra (Fig. 5b,c) of Cr2p and Ti2p show that the chemical state of Ti is tetravalent and Cr is trivalent for both the smooth and hierarchical Cr-doped titania particles. The position of Ti2p peaks in the Cr-doped titania slightly shift towards higher binding energies compared to that of the pure titania, implying a little influence of local chemical state by Cr-doping.[38]

Although the composition and crystal structure are similar for the hierarchical and the smooth Cr-doped titania particles, the hierarchical particles exhibit higher specific surface areas according to N_2 adsorption–desorption isotherms (Fig. S2, ESI†). The BET surface area (S_{BET}) of the hierarchical Cr-doped titania particles is 65 m^2/g, which is about 13 times as high as that of the smooth Cr-doped titania particles (S_{BET} = 5.3 m^2/g). Similarly, the S_{BET} of the hierarchical pure titania particles is also higher compared to the smooth pure titania particles. This can be attributed to the presence of high surface area nanostructures on the hierarchical particles.

Electrorheological properties

Fig. 6a and b show the flow curves of shear stress and shear viscosity *vs.* shear rate measured by the CSR mode for the suspensions containing 10 vol% hierarchical and smooth Cr-doped titania particles, respectively. In the absence of an electric field, both suspensions show a shear-thinning behavior at low shear rate regions and a Newtonian fluid behavior at high shear rate regions. The no-field viscosity of the hierarchical Cr-doped titania suspension is close to 0.30 Pas, which is higher than that of the smooth Cr-doped titania suspension (0.26 Pas). This is likely because the sea-urchin-like hierarchical particles, with a high surface area, have larger interparticle friction and drag forces compared to the smooth particles. When an electric field is applied, the suspensions each exhibit a shear stress or viscosity elevation, and the yield phenomena can be found. However, it is

View Article Online

Published on 22 September 2009. Downloaded by Pennsylvania State University on 16/09/2016 13:48:09.

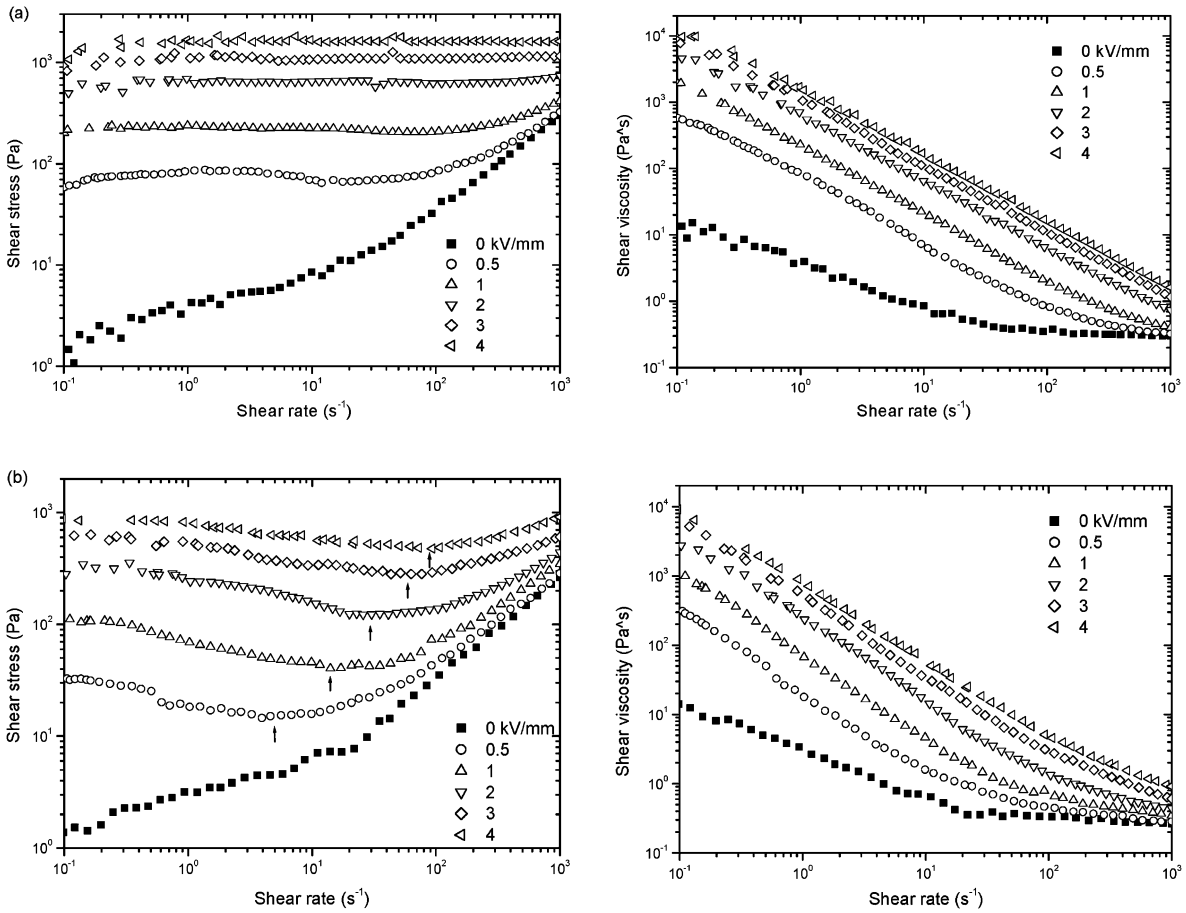

Fig. 6 Flow curves of shear stress and shear viscosity as a function of shear rate measured by the CSR mode for the suspensions: (a) hierarchical Cr-doped titania particles; (b) smooth Cr-doped titania particles. (T = 23 °C, particle concentration = 10 vol%).

interesting that the yield stress (approximately obtained at low shear rates) or ER efficiency (defined by $(\tau_E - \tau_0)/\tau_0$, where τ_E is the shear stress with an electric field and τ_0 is the shear stress without electric field, respectively) for the suspension of hierarchical Cr-doped titania is much higher than that of the corresponding suspension of smooth Cr-doped titania at equal electric fields. The typical ER efficiency of the hierarchical Cr-doped titania suspension is 159 (10 s^{-1}) and 37 (100 s^{-1}) at 4 kV/mm, which is significantly higher than that of the smooth Cr-doped titania suspension (85 at 10 s^{-1} and 15 at 100 s^{-1}). At 1000 s^{-1}, the ER efficiency of the hierarchical Cr-doped titania suspension still reaches 4.6 at 4 kV/mm, while that of the smooth Cr-doped titania suspension is 2.5. Furthermore, from the flow curves it is seen that the shear stress of the hierarchical Cr-doped titania suspension maintains a wide plateau level in the measured shear rate regions. But the plateau region of shear stress for the smooth Cr-doped titania suspension is narrow and the shear stress as a function of shear rate decreases to a minimum value (see arrows in Fig. 6b) and then increases with shear rate. The analogical result of shear stress with shear rate decrease to a minimum was also observed in other ER fluids.[20d,39] It is known that the rheological behavior of ER fluids is influenced mainly by the changes (*i.e.* reorganization and destruction) of ER structures.[20d,31e,39] These structure changes were further dominated by the completion between the electrostatic interactions among particles induced by electric fields and the hydrodynamic interactions induced by shear fields. The electrostatic interactions were responsible for the reorganization of ER structures and hindered the flow, while the hydrodynamic interactions tended to destroy ER structures and promoted the flow. At low shear rate regions, the hydrodynamic interactions were small and the electrostatic interactions dominated the flow. As the shear rate increases, the hydrodynamic interactions became stronger and gradually overcame the electrostatic interactions, so that the destruction rate of ER structure became faster than the reorganization rate and thus the shear stress decreased. Therefore, the different rheological curves also reveal that the structuring process of the hierarchical Cr-doped titania suspension is different from that of the smooth Cr-doped titania suspension. The flow curves with the appearance of narrow plateau region or of shear stress decrease to a minimum value, for the smooth Cr-doped TiO_2 suspension, reveal that the destruction rate of ER structures becomes faster than the reorganization rate. However, the more stable shear stress level in the wide shear rate region for the hierarchical particle suspension indicates that the ER structures formed by hierarchical particles is more stable, further hinting at the stronger interactions between the hierarchical Cr-doped titania particles.

The yield stress plotted as a function of electric field strength is presented in Fig. 7. It is clearly seen that not only Cr-doping

 This journal is © The Royal Society of Chemistry 2009

View Article Online

Published on 22 September 2009. Downloaded by Pennsylvania State University on 16/09/2016 13:48:09.

increases the yield stress but also introducing a sea-urchin-like nanostructure onto titania particles further enhances it. For example, the yield stress of the hierarchical Cr-doped titania suspension is about 1.67 kPa at 4 kV/mm, which is roughly twice as high as that of the smooth Cr-doped titania suspension (0.89 kPa), 3.5 times as high as that of the hierarchical pure titania suspension (0.48 kPa), and 13 times as high as that of the smooth pure titania suspension (0.13 kPa). According to the structural characterizations above, it has been known that the chemical composition and crystal structure of the hierarchical particles are similar to those of the smooth particles, but their particle morphology is significantly different. So, it is presumed that the enhanced ER effect may be mainly related to the morphology of particles (although there is a small difference in the outer diameter of particles between the hierarchical and smooth ones, no effect of particle size on the ER properties is expected since this effect is negligible for the small difference in particle size).[40] To further clarify this, two additional Cr-doped titania samples with changed surface morphologies were prepared. For one, the prepared process is similar to the hierarchical Cr-doped titania particles described in the Experimental Section except that the solvothermal reaction is decreased to 120 °C for 8 h. By this process, Cr-doped titania particles with a less well-developed sea-urchin-like nanostructure (*i.e.*, with shorter and thinner titania nanorods; see SEM in Fig. S3a, ESI†) are prepared. For another, the prepared process is also similar to the hierarchical Cr-doped titania particles but a small amount of surfactant is added. Then Cr-doped titania particles without an urchin-like nanostructure are obtained. But the surface of such particles is relatively coarse compared to the smooth Cr-doped titania particles (see SEM in Fig. S3b, ESI†). The rheological results (see Fig. 8) show that the yield stress of the surface-coarsened Cr-doped titania suspension is close to that of the smooth Cr-doped titania suspension, while the yield stress of the less well-developed hierarchical Cr-doped titania suspension is increased. This clearly indicates that introducing an urchin-like nanostructure onto the surface of Cr-doped titania particles does play an important role in the enhancement of the ER effect. In terms of the dielectric analysis and microscopic observation, two possible reasons are responsible for this ER enhancement including (1) improved interfacial polarization due to the high surface area of sea-urchin-like nanostructures, and (2) increased interparticle friction and mechanical cohesion due to the interlocking effect of the sea-urchin-like nanostructures on ER particles. We will discuss this based on the dielectric measurement and microscopic observation of ER structures in the next section.

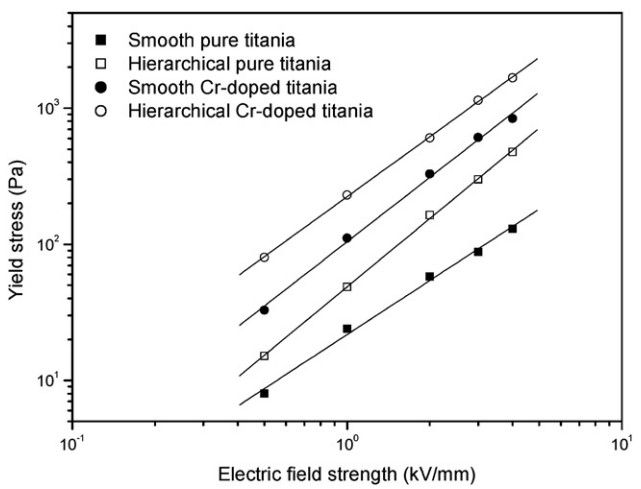

Fig. 7 Yield stress plotted as a function of electric field strengths for different suspensions. (T = 23 °C, 10 vol%).

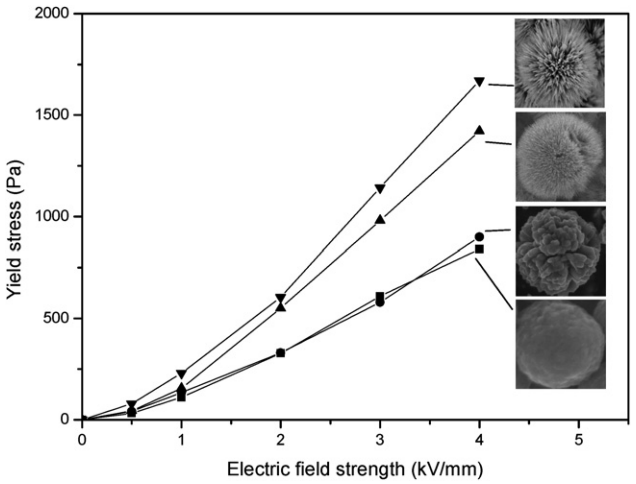

Fig. 8 Yield stress as a function of electric field strengths for the suspensions of Cr-doped titania particles with different surface morphologies (■: smooth Cr-doped titania; ●: surface-coarsened Cr-doped titania without sea-urchin-like nanostructure; ▲: hierarchical Cr-doped titania with a less well-developed sea-urchin-like nanostructure; ▼: hierarchical Cr-doped titania). (T = 23 °C, 10 vol%.)

On the other hand, since the ER fluids under electric fields often display a viscoelastic behavior, the dynamic rheological measurements are also used to examine the ER properties. Fig. 9 shows the frequency dependence of storage modulus (G') and loss modulus (G'') of the suspensions at a low stress of 30 Pa in the linear regions under different electric fields. It is seen that the suspensions each show a solid-like behavior, *i.e.* G' is substantially larger than G'', and G' remains at a near plateau over a broad frequency range. The storage modulus of the hierarchical Cr-doped titania suspension is much larger than that of the smooth Cr-doped titania suspension at an equal electric field. Meanwhile, the larger storage modulus is also confirmed for the hierarchical pure titania suspension (Fig. S4, ESI†). It has been accepted for ER fluids that the plateau of the frequency-dependent curves of viscoelastic functions is a characteristic of aligned 3D microstructures under electric fields, which is sufficiently strong to transmit the elastic forces through particle–particle bonds.[29] Therefore, the larger storage modulus of the hierarchical titania suspension reflects its higher solidified level (rigidity) or ER effect, which is also in good accordance with its higher yield stress.

As the applied stress increases and then exceeds the yield point, the rupture behavior is shown in the stress-dependent curves of moduli. Fig. 10 presents the stress dependence of moduli of the suspensions at a frequency of 0.5 Hz under different electric fields. From the dynamic moduli, some significant differences between the smooth Cr-doped titania and the hierarchical Cr-doped titania suspensions are noted. At low stresses, the hierarchical Cr-doped titania suspension is harder than the smooth Cr-doped titania suspension by showing the higher plateau of G'. After the stress exceeds the yield point, the hierarchical Cr-doped

View Article Online

Published on 22 September 2009. Downloaded by Pennsylvania State University on 16/09/2016 13:48:09.

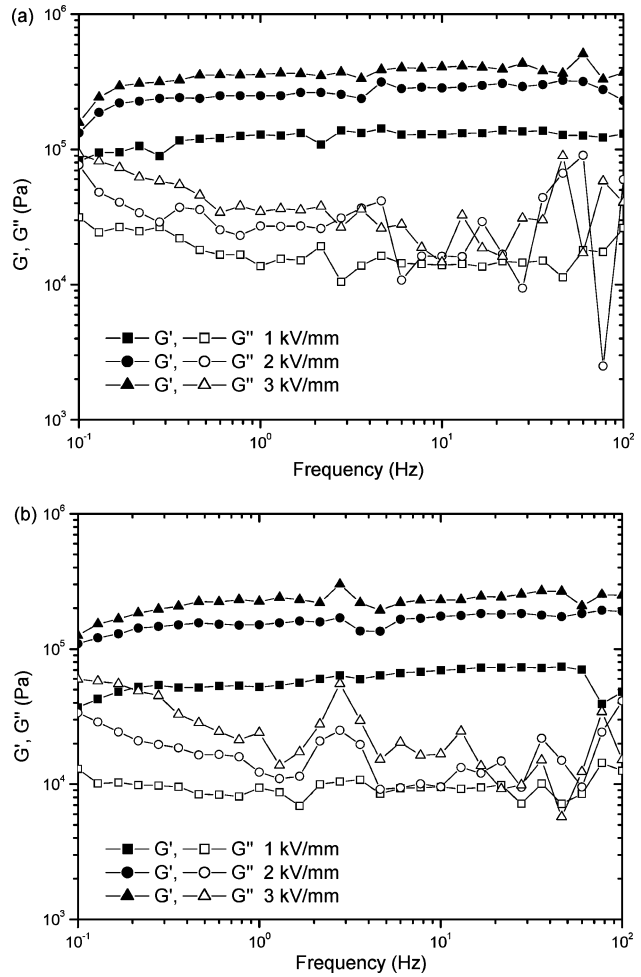

Fig. 9 Frequency dependence of storage modulus (G') and loss modulus (G'') for the suspensions: (a) hierarchical Cr-doped titania particles; (b) smooth Cr-doped titania particles. (T = 23 °C, 10 vol%.)

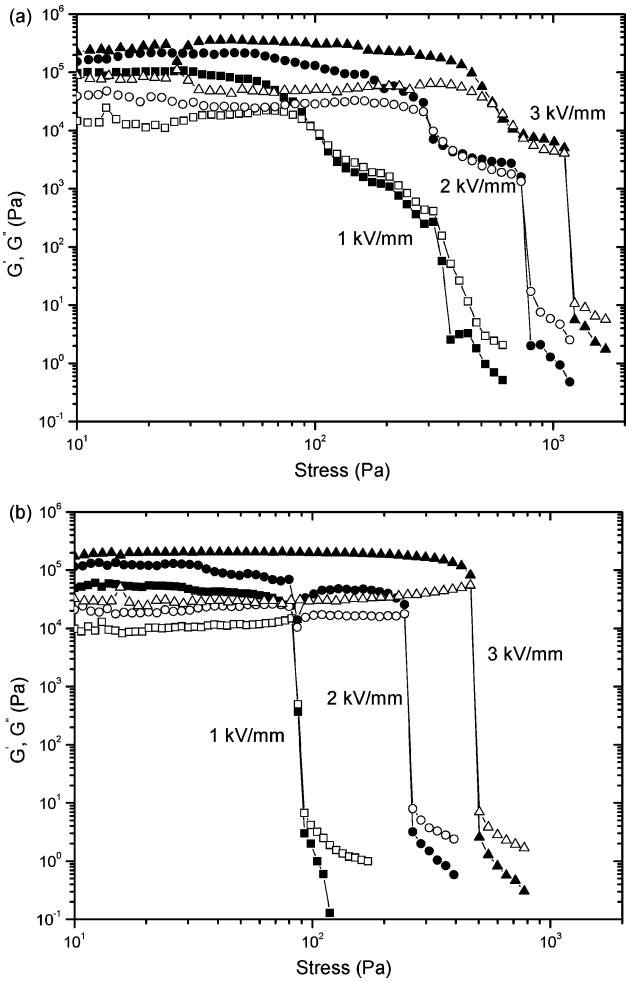

Fig. 10 Stress dependence of storage modulus (G', solid symbol) and loss modulus (G'', open symbol) for the suspensions: (a) hierarchical Cr-doped titania particles; (b) smooth Cr-doped titania particles. (T = 23 °C, 10 vol%.)

titania suspension shows a shoulder-like drop (Fig. 10a) while the smooth Cr-doped titania suspension drops suddenly (Fig. 10b). Similarly, the shoulder-like yield process is also observed in the hierarchical pure titania suspension but not observed in the smooth pure titania suspension (Fig. S5, ESI†). The shoulder-like yield process indicates that the transformation of the hierarchical titania suspension from a solid-like state to a liquid-like state is more gradual than the smooth titania suspension, which further represents a complex structuring process of ER structures induced by shearing fields.[29] This may be related to the morphology of particles, which has influenced interparticle interactions. Therefore, according to the rheological results obtained it can be demonstrated that under electric fields the sea-urchin-like hierarchical titania suspension not only has a higher ER effect but also has a different structuring process from the smooth non-hierarchical titania suspension. To understand the structurally enhanced ER effect, the dielectric properties and aligned ER structures of suspensions are investigated.

Dielectric properties and ER structures

Since the ER effect is induced by an external electric field, the particle polarization is believed to be important and the dielectric properties play a dominant role.[26] It has been proposed that a good ER effect requires that the ER fluids should first have a dielectric relaxation peak of dielectric loss (ε'') within an adequate frequency range of 10^2–10^5 Hz and then have a large dielectric constant difference ($\Delta\varepsilon' = \varepsilon'_{10^2\mathrm{Hz}} - \varepsilon'_{10^5\mathrm{Hz}}$).[26,41] The dielectric relaxation peak was related to the polarization response denoted by the relaxation time ($\tau = \frac{1}{2\pi f_{\max}}$, where $f_{\max}$ is the local frequency of the ε'' peak), while $\Delta\varepsilon'$ was related to the magnitude of achievable polarizability. As the relaxation time got smaller and the higher $\Delta\varepsilon'$ within this frequency range was applied, a higher ER enhancement would be achieved. Table 1 recapitulates the dielectric data of the suspensions according to the frequency-dependent spectra of real (ε') and imaginary (ε'') parts of complex permittivity. There is not a loss peak in the pure titania suspensions and the $\Delta\varepsilon'$ is very small. This inferior dielectric property is the reason for a poor ER effect of the pure titania suspension.[28] Doping with Cr ions increases the interfacial polarization of the suspension, which can be reflected by the loss peak at about 60 Hz and the larger $\Delta\varepsilon'$. This maybe resulted from the increase of defects and impurities due to doping.[17c] In

 This journal is © The Royal Society of Chemistry 2009

View Article Online

Published on 22 September 2009. Downloaded by Pennsylvania State University on 16/09/2016 13:48:09.

comparison with the smooth Cr-doped titania suspension, the loss peak of the hierarchical Cr-doped titania suspension shifts to 150 Hz and its $\Delta\varepsilon'$ becomes larger, indicating that introducing the sea-urchin-like nanostructure onto the Cr-doped titania particles to some extent enhances the interfacial polarization. This is likely ascribed to the larger surface area of the hierarchical Cr-doped titania particles compared to the smooth ones because it has been reported that the suspension containing particles with a high surface area often showed an increased interfacial polarization.[25c,d,42] Therefore, according to the proposed mechanism, this improved polarization may be one factor to induce the enhancement of the ER effect of the hierarchical Cr-doped titania suspension.

In addition, knowing ER structures under electric and shearing fields, in particular the interparticle interaction, is also essential to understand the ER properties.[12c,43] The structure of the suspensions between the electrodes under the oscillatory shear with a small strain is shown in Fig. 11. Note that the small strain is able to deform the structure but not destroy it. For the smooth Cr-doped titania suspension, the particles align and form a column-like structure (Fig. 11 A-a, one column size is about 0.1–0.3 mm) after the 3 kV/mm electric field is applied. When the strain is used, the columns incline with an oscillatory motion (Fig. 11 A-b). After the oscillatory shear is removed, the columns stop swinging but the column size (Fig. 11 A-c) almost remains unchanged. For the suspension of hierarchical doped titania particles, however, it is noted that the aligned structure is rather different from that in the suspension of smooth particles. When the electric field is applied, the particles quickly form a dense fiber-like network structure (Fig. 11 B-a) and no clear column-like structure is observed even if the electric field has been applied for 300 s. But, it is interesting that the column-like structure is gradually formed (Fig. 11 B-c) and thickened (Fig. 11 B-e) when the suspension is subjected to oscillatory shearing. These reflect that the hierarchical particle suspension do have a different structuring process with the smooth particle suspension, and the shearing field seems to promote further aggregation of the hierarchical particles. Therefore, it can be presumably concluded that the differences in rheological properties between the smooth and hierarchical Cr-doped titania suspensions are attributed to their different structuring processes of ER structures, which may be further related to the influences of the unique morphology of particles on interparticle interactions. It is easy to understand in a qualitative way that, in the suspension of smooth non-hierarchical particles, the influences of interparticle friction and mechanical cohesion on the ER structures and rheological properties are negligible in comparison with the other forces (such as electrostatic interactions and hydrodynamic interactions).[44] However, in the suspension of sea-urchin-like hierarchical particles, the interparticle friction and mechanical cohesion might have been significantly increased due to the interlocking effect of the rough surface and then have played a role in the ER structures and rheological properties. In particular, under electric fields, the interparticle friction and mechanical cohesion between the sea-urchin-like particles may be further increased because of the enhancement of interlocking effects as shown by the SEM in Fig. 11B-f. Obviously, the increase of interparticle friction and mechanical cohesion is beneficial for the resistance of the flow of suspensions.[12b,44] As a consequence, the resulting yield stress or ER effect of the sea-urchin-like hierarchical titania suspension is enhanced by the combined effects of the electric attractive force and the

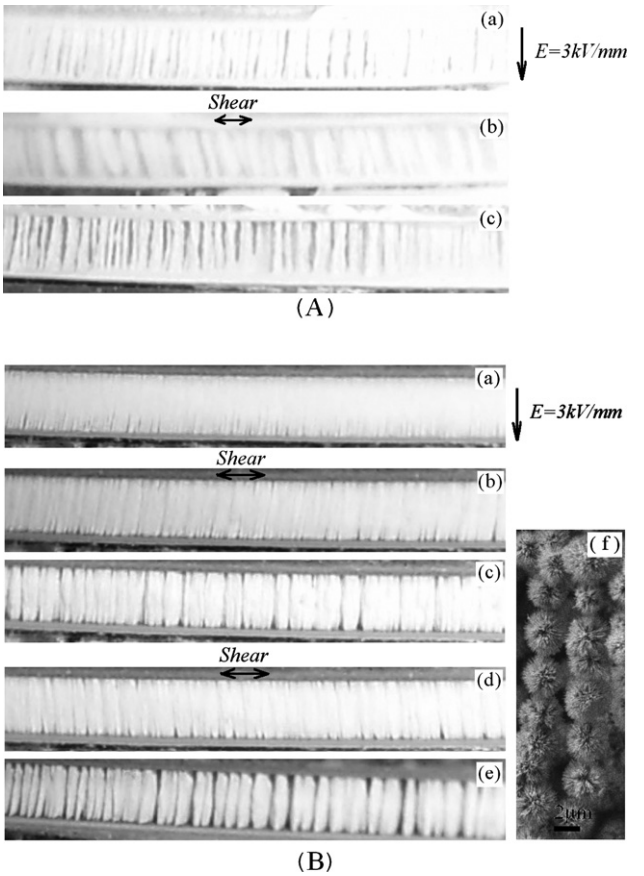

Fig. 11 (A) ER structures of the smooth Cr-doped titania suspension between the electrodes: (a) after 3 kV/mm electric field is applied for 120 s under no shearing, (b) when the shearing is applied, (c) after the shearing is stopped; (B) ER structures of the hierarchical Cr-doped titania suspension between the electrodes: (a) after 3 kV/mm electric field is applied for 300 s under no shearing, (b) when the shearing is applied, (c) after the shearing is stopped, (d) when the shearing is applied again, (e) after the second shearing is stopped, (f) SEM image of the aligned chains of hierarchical doped titania particles. (The gap between electrodes was fixed to 1.0 mm, T = 23 °C, 10 vol%.)

Table 1 Dielectric data of the suspensions containing smooth and hierarchical titania particles

Sample	$\varepsilon'_{10^2\mathrm{Hz}}$	$\varepsilon'_{10^5\mathrm{Hz}}$	$\Delta\varepsilon'^{a}$	f_{max} (Hz)^{b}	ε''^{c}
Smooth pure titania	3.48	3.30	0.18	—	0.051
Hierarchical pure titania	3.95	3.37	0.58	—	0.160
Smooth Cr-doped titania	5.46	3.50	1.96	60	0.607
Hierarchical Cr-doped titania	5.85	3.64	2.21	150	0.758
Silicone oil used	2.84	2.83	—	—	<0.001

[a] Dielectric constant difference, calculated by $\Delta\varepsilon' = \varepsilon'_{10^2\mathrm{Hz}} - \varepsilon'_{10^5\mathrm{Hz}}$. [b] The local frequency of peak of dielectric loss factor ε'' within 10^2–10^5 Hz. [c] The magnitude of dielectric loss factor for the Cr-doped titania suspensions is at the peak frequency, while for the pure titania suspensions and silicone oil a frequency of 60 Hz was used.

View Article Online

Published on 22 September 2009. Downloaded by Pennsylvania State University on 16/09/2016 13:48:09.

interparticle friction and mechanical cohesion. At the same time, the increased interparticle friction and cohesion or the interlocking effect of sea-urchin-like hierarchical particles might have made the attraction and separation between particles under electric and shearing fields become more complex in comparison with the smooth particles, which result in their significantly different structuring process and rheological properties. Therefore, in terms of the present experimental results, the enhancement of ER effect of the sea-urchin-like hierarchical Cr-doped titania suspension is likely attributed to the combined effect of the improved interfacial polarization and the increased interparticle friction and mechanical cohesion due to the introduction of unique sea-urchin-like nano-morphology onto ER microparticles.

Conclusions

In conclusion, we have developed a novel ER suspension composed of Cr-doped titania particles that have a unique sea-urchin-like hierarchical morphology. The structural analysis revealed that the hierarchical Cr-doped titania particles were nearly monodisperse and consisted of high-density rutile Cr-doped titania nanorods with a diameter of 20–30 nm assembled radially on the surfaces of the particles. The Cr ions were doped into titania with a trivalent state. The N_2 adsorption test showed the specific surface area of the hierarchical Cr-doped titania particles was close to 65 m^2/g, which was 13 times as high as that of the smooth Cr-doped titania particles whose crystal structure and composition were similar to those of the hierarchical ones. The rheological experiments showed that the suspension of hierarchical Cr-doped titania possessed a distinctly enhanced ER effect compared to the corresponding suspension of smooth Cr-doped titania particles. Its yield stress was approximately twice as high as that of the smooth Cr-doped titania suspension, 3.5 times as high as that of the hierarchical pure titania suspension, and 13 times as high as that of the smooth pure titania suspension. Furthermore, the rheological properties and structuring processes of ER structures of the hierarchical titania suspension were also different from those of the smooth titania suspension. The shear stress of the hierarchical Cr-doped titania suspension maintained a stable level in the whole shear rate region, while the shear stress of the smooth Cr-doped titania suspension as a function of shear rate tended to decrease to a minimum value and then increase with shear rate. In the dynamic shear, the stress-dependent curves of the moduli of the hierarchical titania suspension exhibited a shoulder-like drop, which was also different from the sudden drop of moduli of the smooth titania suspension at the yield point. The investigations on the dielectric properties and microscopic ER structures indicated that introducing sea-urchin-like nanostructured morphology onto titania microparticles not only improved the interfacial polarization but also might influence the interparticle interaction (such as increased interparticle friction and mechanical cohesion) due to the interlocking effect of the sea-urchin-like nanostructures. Their combined effects might be responsible for the enhancement of an ER effect of the Cr-doped titania particles with a unique sea-urchin-like morphology. At the same time, the increased interparticle friction and cohesion or the interlocking effect of urchin-like hierarchical particles might have made the interparticle interaction became more complex in comparison with the smooth particles, which results in a significantly different structuring process and rheological properties between the smooth particle suspension and the hierarchical particle suspension. The results obtained in the present paper possibly provide a route for the preparation of a high-performance ER suspension.

Acknowledgements

We are grateful to the help from Dr Yan L. Ai on XRD, Dr Xiao C. Chen on TEM/EDS and XPS, and Mr Zhuang Miao on SEM measurements. This work is supported by the National Natural Science Foundation of China (No. 50602036), NPU Foundation for Fundamental Research (No. WO18101), and Yingcai program (No. 05XE0129).

References

1 C. Burda, X. B. Chen, R. Narayaman and M. A. El-Sayed, *Chem. Rev.*, 2005, **105**, 1025.
2 Z. L. Wang and J. H. Song, *Science*, 2006, **312**, 242.
3 L. Zhang and Y. J. Zhu, *J. Phys. Chem. C*, 2008, **112**, 16764.
4 X. F. Gao and L. Jiang, *Nature*, 2004, **432**, 36.
5 (*a*) K. Autumn, Y. A. Liang, S. T. Hsieh, W. Zesch, W. P. Chan, T. W. Kenny, R. Fearing and R. J. Full, *Nature*, 2000, **405**, 681; (*b*) K. Autumn, M. Sitti, Y. A. Liang, A. M. Peattie, W. R. Hansen, S. Sponberg, T. W. Kenny, R. Fearing, J. N. Israelachvili and R. J. Full, *Proc. Natl. Acad. Sci. U. S. A.*, 2002, **99**, 12252.
6 L. H. Ge, S. Sethi, L. J. Ci, P. M. Ajayan and A. Dhinojwala, *Proc. Natl. Acad. Sci. U. S. A.*, 2007, **104**, 10792.
7 (*a*) S. L. Xiong, B. J. Xi, C. W. Wang, D. C. Xu, X. M. Feng, Z. C. Zhu and Y. T. Qian, *Adv. Funct. Mater.*, 2007, **17**, 2728; (*b*) F. Lu, W. P. Cai and Y. G. Zhang, *Adv. Funct. Mater.*, 2008, **18**, 1047.
8 (*a*) Z. L. Wang, *J. Phys.: Condens. Matter*, 2004, **16**, R829; (*b*) S. W. Cao, Y. J. Zhu, M. Y. Ma and L. Zhang, *J. Phys. Chem. C*, 2008, **112**, 1851.
9 D. O'Dwyer, V. Navas, E. Lavayen, M. A. Benavente, G. Santa Ana, S. González, B. Newcomb and C. M. Sotomayor Torres, *Chem. Mater.*, 2006, **18**, 3016.
10 (*a*) R. C. Kanu and M. T. Shaw, *J. Rheol.*, 1998, **42**, 657; (*b*) M. Shen, J. G. Cao, H. T. Xue, J. P. Huang and L. W. Zhou, *Chem. Phys. Lett.*, 2006, **423**, 165.
11 (*a*) K. Yatsuzuka, K. Miura, N. Kuramoto and K. Asano, *IEEE Trans. IAS.*, 1995, **31**, 457; (*b*) K. Asano, H. Suto and K. Yatsuzuka, *J. Electrost.*, 1997, **40–41**, 573.
12 (*a*) H. T. Pu and F. J. Jiang, *Nanotechnology*, 2005, **16**, 1486; (*b*) M. T. López-López, G. Vertelov, G. Bossis, P. Kuzhir and J. D. G. Durán, *J. Mater. Chem.*, 2007, **17**, 3839; (*c*) R. C. Bell, J. O. Karli, A. N. Vavreck, D. T. Zimmerman, G. T. Ngatu and N. M. Wereley, *Smart Mater. Struct.*, 2008, **17**, 015028.
13 W. Wen, X. Huang and P. Sheng, *Soft Matter*, 2008, **4**, 200.
14 (*a*) H. Block and J. P. Kelly, *J. Phys. D: Appl. Phys.*, 1988, **21**, 1661; (*b*) A. P. Gast and C. F. Zukowski, *Adv. Colloid Interface Sci.*, 1989, **30**, 153; (*c*) J. P. Coulter, K. D. Weiss and J. D. Carlson, *J. Intell. Mater. Syst. Struct.*, 1993, **4**, 248; (*d*) T. Hao, *Adv. Mater.*, 2001, **13**, 1847.
15 (*a*) X. P. Zhao and J. B. Yin, *J. Ind. Eng. Chem.*, 2006, **12**, 184; (*b*) X. P. Zhao, J. B. Yin and H. Tang, in *Smart Materials and Structures: New Research*, ed. P. L. Reece, Nova Science Publishing, 2007, pp. 1–66.
16 (*a*) F. E. Filisko and L. H. Radzilowski, *J. Rheol.*, 1990, **34**, 539; (*b*) H. Conrad, A. F. Sprecher, Y. Choi and Y. Chen, *J. Rheol.*, 1991, **35**, 1393; (*c*) Y. Tian, Y. G. Meng and S. Z. Wen, *J. Appl. Phys.*, 2001, **90**, 493.
17 (*a*) X. P. Zhao, J. B. Yin and L. Q. Xiang. Chinese Pat., 99115944.6, 1999; (*b*) X. P. Zhao and J. B. Yin, *Chem. Mater.*, 2002, **14**, 2258; (*c*) J. B. Yin and X. P. Zhao, *Chem. Mater.*, 2004, **16**, 321.
18 (*a*) W. Wen, W. Y. Tam and P. Sheng, *J. Mater. Sci. Lett.*, 1998, **17**, 419; (*b*) Y. L. Zhang, K. Q. Lu, G. H. Rao, Y. Tian, S. H. Zhang and

 This journal is © The Royal Society of Chemistry 2009

View Article Online

Published on 22 September 2009. Downloaded by Pennsylvania State University on 16/09/2016 13:48:09.

J. K. Liang, *Appl. Phys. Lett.*, 2002, **80**, 888; (*c*) J. B. Yin and X. P. Zhao, *J. Solid State Chem.*, 2004, **177**, 3650.
19 (*a*) Y. Z. Xu and R. F. Liang, *J. Rheol.*, 1991, **35**, 1355; (*b*) R. Sakurai, H. See and T. Satio, *J. Rheol.*, 1996, **40**, 395; (*c*) K. Negita, Y. Misono, T. Yamaguchi and J. Shinagawa, *J. Colloid Interface Sci.*, 2008, **321**, 452; (*d*) Y. P. Qiao and X. P. Zhao, *Colloid Surf. A*, 2009, **340**, 33.
20 (*a*) H. Block and J. P. Kelly, UK Pat., 217051B, 1986; (*b*) H. Block, J. P. Kelly, A. Qin and T. Watson, *Langmuir*, 1990, **6**, 6; (*c*) Z. W. Gao and X. P. Zhao, *Polymer*, 2003, **44**, 4519; (*d*) M. S. Cho, J. W. Kim, H. J. Choi and M. S. Jhon, *Polym. Adv. Technol.*, 2005, **16**, 352; (*e*) O. Quadrat and J. Stejskal, *J. Ind. Eng. Chem.*, 2006, **12**, 352; (*f*) D. H. Kim and Y. D. Kim, *J. Ind. Eng. Chem.*, 2007, **13**, 879.
21 (*a*) W. Y. Tam, G. H. Yi, W. Wen, H. Ma, M. M. T. Loy and P. Sheng, *Phys. Rev. Lett.*, 1997, **78**, 2987; (*b*) M. Knishi, T. Nagashima and Y. Asako, in *Proceedings of the 6th International Conference on ERF and MRS*, ed. M. Nakano and K. Koyama, World Scientific of Singapore, 1998, p. 17; (*c*) C. R. Luo, H. Tang and X. P. Zhao, *Int. J. Mod. Phys. B*, 2001, **15**, 672; (*d*) M. S. Cho, Y. H. Cho, H. J. Choi and M. S. Jhon, *Langmuir*, 2003, **19**, 5875.
22 (*a*) H. J. Choi, J. W. Kim, M. H. Noh, D. C. Lee, M. S. Suh, M. J. Shin and M. S. Jhon, *J. Mater. Sci. Lett.*, 1999, **18**, 1505; (*b*) J. Lu and X. P. Zhao, *J. Mater. Res.*, 2002, **17**, 1513; (*c*) X. P. Zhao and X. Duan, *J. Colloid Interface Sci.*, 2002, **251**, 376; (*d*) L. Q. Xiang and X. P. Zhao, *J. Mater. Chem.*, 2003, **13**, 1529.
23 (*a*) H.-J. Jin, H. J. Choi, S. H. Yoon, S. J. Myung and S. E. Shim, *Chem. Mater.*, 2005, **17**, 4034; (*b*) I. S. Lee, S. H. Yoon, H.-J. Jin and H. J. Choi, *Diamond Relat. Mater.*, 2006, **15**, 1094; (*c*) S. J. Han, B. Kim and K. D. Suh, *Mater. Lett.*, 2007, **61**, 3995; (*d*) H. J. Choi and M. S. Jhon, *Soft Matter*, 2009, **5**, 1562.
24 (*a*) H. J. Choi, M. S. Cho, Y. K. Kang and W. S. Ahn, *Microporous Mesoporous Mater.*, 2000, **39**, 19; (*b*) M. S. Cho, H. J. Choi and K. Y. Kim, *Macromol. Rapid Commun.*, 2002, **23**, 713; (*c*) M. S. Cho, H. J. Choi and W. S. Ahn, *Langmuir*, 2004, **20**, 202.
25 (*a*) X. P. Zhao and J. B. Yin, Chinese Pat., 02114691.8, 2002; (*b*) J. B. Yin and X. P. Zhao, *Chem. Mater.*, 2002, **14**, 4633; (*c*) J. B. Yin and X. P. Zhao, *Chem. Phys. Lett.*, 2004, **398**, 393; (*d*) J. B. Yin and X. P. Zhao, *J. Phys. Chem. B*, 2006, **110**, 12916.
26 H. Block and P. Rattay, in *Progress in Electrorheology*, ed. K. O. Havelka and F. E. Filisko, Plenum Press of New York, 1995, pp. 19–42.
27 (*a*) F. E. Filisko, in *Progress in Electrorheology*, ed. K. O. Havelka and F. E. Filisko, Plenum Press of New York, 1995, pp 3–18; (*b*) P. Atten, J.-N. Foulc and N. Felici, *Int. J. Mod. Phys. B*, 1994, **8**, 2731; (*c*) K. Negita and Y. Osawa, *Phys. Rev. E: Stat., Nonlinear, Soft Matter Phys.*, 1995, **52**, 1934; (*d*) Y. Komoda, T. N. Rao and A. Fujishima, *Langmuir*, 1997, **13**, 1371; (*e*) Y. Komoda, N. Sakai and T. N. Rao, *Langmuir*, 1998, **14**, 1081; (*f*) Z. Y. Qiu, H. Zhang, Y. Tang and L. W. Zhou, In *Proceeding of 6th International Conference on ER Fluids and MR Suspensions and Their Applications*, ed. M. Nakano and K. Koyama, World Scientific of Singapore, 1998, p. 197.
28 (*a*) T. Hao, *Appl. Phys. Lett.*, 1997, **70**, 1956; (*b*) J. B. Yin and X. P. Zhao, *J. Phys. D: Appl. Phys.*, 2001, **34**, 2063.
29 (*a*) Y. Otsubo, *Colloids Surf., A*, 1999, **153**, 459; (*b*) K. Tsuda, Y. Takeda, H. Ogura and Y. Otsubo, *Colloids Surf., A*, 2007, **299**, 262.
30 (*a*) J. B. Yin and X. P. Zhao, *Nanotechnology*, 2006, **17**, 192; (*b*) K. Lozano, C. Hernandez, T. W. Petty, M. B. Sigman and B. Korgel, *J. Colloid Interface Sci.*, 2006, **297**, 618; (*c*) C. Lin and J. W. Shan, *Phys. Fluids*, 2007, **19**, 121702; (*d*) J. B. Yin, X. P. Zhao, X. Xia, L. Q. Xiang and Y. P. Qiao, *Polymer*, 2008, **49**, 4413; (*e*) J. B. Yin and X. P. Zhao, *Colloids Surf., A*, 2008, **329**, 153.
31 (*a*) W. J. Wen, X. X. Huang, S. H. Yang, K. Q. Lu and P. Sheng, *Nat. Mater.*, 2003, **2**, 727; (*b*) K. Q. Lu, R. Shen, X. Z. Wang, G. Sun and W. J. Wen, *Int. J. Mod. Phys. B*, 2005, **19**, 1065; (*c*) G. J. Cao, M. Shen and L. W. Zhou, *J. Solid State Chem.*, 2006, **179**, 1565; (*d*) Y. P. Qiao, J. B. Yin and X. P. Zhao, *Smart Mater. Struct.*, 2007, **16**, 332; (*e*) J. Y. Hong, E. Kwon and J. Jang, *Soft Matter*, 2009, **5**, 951.
32 (*a*) W. J. Wen, X. X. Huang and P. Sheng, *Appl. Phys. Lett.*, 2004, **85**, 299; (*b*) B. X. Wang, Y. Zhao and X. P. Zhao, *Colloids Surf., A*, 2007, **295**, 27; (*c*) X. Q. Gong, J. B. Wu, X. X. Huang, W. J. Wen and P. Sheng, *Nanotechnology*, 2008, **19**, 165602; (*d*) Y. Lu, R. Shen, X. Z. Wang, G. Sun and K. Q. Lu, *Smart Mater. Struct.*, 2009, **18**, 025012.
33 (*a*) G. M. Whitesides and B. Grzybowski, *Science*, 2002, **295**, 2418; (*b*) G. J. de A. A. Soler-Illia, C. Sanchez, B. Lebeau and J. Patarin, *Chem. Rev.*, 2002, **102**, 4093.
34 B. X. Wang and X. P. Zhao, *Adv. Funct. Mater.*, 2005, **15**, 1815.
35 X. P. Zhao, J. B. Yin, L. Q. Xiang and X. Xiang, Chinese Pat., 200810017722.2, 2008.
36 (*a*) A. M. Venezia, L. Palmisano and M. Schiavello, *J. Solid State Chem.*, 1995, **114**, 364; (*b*) R. K. Sharma, M. C. Bhatnagar and G. L. Sharma, *Sens. Actuators, B*, 1997, **45**, 209.
37 M. Valigi, D. Gazzoli, P. Natale and P. Porta, *Gazz. Chim. Ztal.*, 1986, **116**, 391.
38 K. Nagaveni, M. S. Hegde, N. Ravishankar, G. N. Subbanna and G. Madras, *Langmuir*, 2004, **20**, 2900.
39 (*a*) Q. Cheng, V. Pavlinek, A. Lengalova, C. Li, T. Belza and P. Saha, *Microporous Mesoporous Mater.*, 2006, **94**, 193; (*b*) I. S. Lee, M. S. Cho and H. J. Choi, *Polymer*, 2005, **46**, 1317; (*c*) J. W. Kim, F. Liu, H. J. Choi, S. H. Hong and J. Joo, *Polymer*, 2003, **44**, 289; (*d*) W. H. Jang, J. W. Kim, H. J. Choi and M. S. Jhon, *Colloid Polym. Sci.*, 2001, **279**, 823.
40 G. Bossis, N. Kchit, P. Kuzhir, M. T. López-López, A. Meunier, in *11th International Conference on Electrorheological Fluids and Magnetorheological Suspensions*, ed. S. Odenbach and D. Borin, Technische Universität Dresden, Dresden, 2008.
41 (*a*) T. Hao, A. Kawai and F. Ikazaki, *Langmuir*, 1998, **14**, 1256; (*b*) F. Ikazaki, A. Kawai, K. Uchida, T. Kawakami, K. Edmura, K. Sakurai, H. Anzai and Y. Asako, *J. Phys. D: Appl. Phys.*, 1998, **31**, 336; (*c*) A. Kawai, Y. Ide, A. Inoue and F. Ikzaki, *J. Chem. Phys.*, 1998, **109**, 4587.
42 D. R. Gamota, A. W. Schubring, B. L. Mueller and F. E. Filisko, *J. Mater. Res.*, 1996, **11**, 144.
43 (*a*) R. Tao and J. M. Sun, *Phys. Rev. Lett.*, 1991, **67**, 398; (*b*) R. Hanaoka, K. Hotta, H. Anzai, K. Sakurai and S. Kuroda, *Electrical Engineering in Japan*, 2000, **132**, 9.
44 (*a*) M. T. López- López, P. Kuzhir and G. Bossis, *J. Rheol.*, 2009, **53**, 115; (*b*) P. Kuzhir, M. T. López- López and G. Bossis, *J. Rheol.*, 2009, **53**, 127.